Link between fertilization-induced Ca^{2+} oscillations and relief from metaphase II arrest in mammalian eggs: a model based on calmodulin-dependent kinase II activation

Geneviève Dupont*

Unité de Chronobiologie Théorique, Faculté des Sciences, Université Libre de Bruxelles CP231, B-1050 Brussels, Belgium

Abstract

Mammalian eggs are ovulated in metaphase II of meiosis, in a state characterized by high levels of cyclin B and of active maturation promoting factor (MPF). This arrest is mediated by an activity referred to as cytostatic factor (CSF) which prevents the degradation of cyclin. Fertilization triggers a train of Ca^{2+} spikes which is responsible for the decrease in activity of both MPF and CSF. The decline in MPF however much precedes that in CSF. Experimental observations on mammalian eggs indicate that the kinetics of cell cycle resumption much depends on the temporal pattern of the repetitive Ca^{2+} spikes. Here, we propose a theoretical model which accounts for Ca^{2+}-induced relief from metaphase II arrest in mammalian eggs. The model is based on the fact that Ca^{2+}/calmodulin kinase II (CaMKII) activation is the primary event leading to inactivation of both CSF and MPF. To account for experimental observations, it has to be assumed that CaMKII activation affects the level of the active form of the anaphase promoting complex (APC), which initiates the degradation of cyclin, through two pathways characterized by different time scales. Thus, we hypothesize that CaMKII activation by Ca^{2+} leads to the transformation of a mediator protein from a form which stimulates the inactivation of the APC into a form which gradually and indirectly induces the deactivation of CSF. In consequence, a sufficient number of Ca^{2+} spikes first triggers the decrease of MPF, thus allowing the egg to enter in interphase, and later that of CSF. Finally, when CSF is low and when Ca^{2+} oscillations have stopped, the level of MPF can increase again, a phenomenon that would correspond to the first mitosis. This model also accounts for the observed dependence of the time of entry in interphase (marked by the appearance of the pronuclei) on the frequency of Ca^{2+} spikes, as well as for the possible entry in metaphase III arrest, a pathological state of the egg which results from an insufficient activation by Ca^{2+}. This study provides some theoretical prediction as to the time of the first mitosis as a function of the temporal pattern of Ca^{2+} oscillations. © 1998 Elsevier Science B.V. All rights reserved

Keywords: Calcium oscillations; Meiosis; Egg activation; Cell cycle; Frequency-coding; Computer simulation

1. Introduction

In mammals, oscillations in the level of cytosolic

Ca^{2+} is the primary signal responsible for the early development of the egg after fertilization [1–4]. Two hypotheses have been put forward to explain how these Ca^{2+} spikes are triggered by the spermatozoon. First, oscillations could be brought about by a soluble protein, called oscillin, introduced by the

* Corresponding author. Tel.: +32 2 6505787; fax: +32 2 6505767; e-mail: gdupont@ulb.ac.be

sperm in the mature oocyte [5]. Alternatively, the primary trigger could be the activation of an external receptor on the oocyte, which in turn stimulates G-protein [6–8] or tyrosine kinase activity [9] to generate inositol 1,4,5-trisphosphate ($InsP_3$), a universal messenger for Ca^{2+} release from internal stores. As well as the pathway by which fertilization triggers repetitive Ca^{2+} spikes, the signal transduction mechanism between Ca^{2+} increases on one hand, and egg activation and entry into mitosis on the other hand is much investigated; the latter mechanism is the focus of the present study.

Mammalian eggs are ovulated in metaphase II (MII) of meiosis, ready to be fertilized. In this state, the eggs are characterized by high levels of cyclin B and maturation promoting factors (MPF). The latter heterodimer, made of $p34^{cdc2}$ kinase (or cyclin dependent kinase 1) and of a B-type cyclin, is a key component of the cell cycle oscillatory mechanism: the level of MPF indeed peaks at each cellular division. MPF itself possesses a histone H1 kinase activity leading to chromosome condensation, nuclear envelope breakdown and spindle assembly. From a practical point of view, it is interesting to remember that the capacity of the oocytes to phosphorylate histone H1 can be used to estimate their level of MPF. Exit from metaphase and entry into anaphase results from MPF inactivation, which generally occurs through cyclin proteolysis [10]. Cyclin degradation occurs through the formation of an ubiquitin-cyclin complex [11]. The ensuing return to a basal level of MPF activity allows the fertilized egg to enter in interphase, as marked by the formation of pronuclei.

MII arrest is mediated by an activity referred to as cytostatic factor (CSF), a c-mos protooncogene product that prevents ubiquitin-dependent degradation of cyclins, and thus inactivation of MPF. CSF activity was first discovered in *Xenopus* eggs [12,13] and was later shown to be responsible for MII arrest in mammalian eggs as well [14]. Translation of c-mos is induced by progesterone; the level of c-mos protein increases during maturation, reaching a maximum at MII. Then, CSF activity remains at a high stable level that prevents cyclin degradation. Just how CSF restrains the activation of the ubiquitin-dependent proteasome pathway responsible for cyclin degradation remains unclear, but this process probably involves the control of the dynamics of the microtu-

bule network [15–17]. It is known moreover that CSF arrest is mediated by enzymes of the mitogen-activated protein (MAP) kinase family [18]. In consequence, the level of CSF activity can be estimated by assaying the oocytes for their capacity to phosphorylate myelin basic protein (MBP), a well-known substrate for MAP kinases.

Although CSF prevents the degradation of cyclin, the inactivation of CSF itself is not required for the proteolysis of the cyclin subunit of MPF and for the resulting exit from meiotic metaphase. In cytosolic extracts from MII arrested eggs of both amphibians and mammals, MPF is inactivated before CSF [13,14]. However, the time scale appears to be very different in both types of organisms; the lag time between MPF and CSF inactivation is of the order of 10 min in *Xenopus* oocytes [13] but of 3 h in mouse oocytes [14].

Both MPF and CSF can be inactivated by the Ca^{2+}/calmodulin-dependent protein kinase II (CaMKII) upon fertilization. A truncated, constitutively active form of CaMKII indeed suffices to induce cyclin degradation and $p34^{cdc2}$ kinase inactivation in cytosolic extracts from MII-arrested *Xenopus* eggs [19,20]. In the same manner, activation of mouse eggs is significantly delayed in the presence of the calmodulin antagonist W-7 [21].

There is little doubt that the Ca^{2+} rise brought about by fertilization is the primary event responsible for early egg activation. In non-mammalian species, for which *Xenopus* eggs are a good prototype, a large, but unique increase in cytosolic Ca^{2+} is observed at fertilization and suffices to activate the egg. The question thus remains as to the possible function of Ca^{2+} oscillations in CaMKII-mediated activation of mammalian eggs. In a more general context, it has been suggested that the repetitive rises in cytosolic Ca^{2+} observed in a large variety of cell types are a means by which information carried by the extracellular signal is conveyed into the cell interior in a frequency-encoded manner [22–25]. These studies, which do not focus on any specific signalling system, remain rather speculative. In the case of mammalian fertilization, the role of Ca^{2+} oscillations has been experimentally approached in great detail, allowing for the development of a specific theoretical model.

Sophisticated methods of cell membrane electroporation by electrical field stimulation allow one to

study the effect of submitting mature, unfertilized mammalian eggs to repetitive Ca^{2+} spikes of various periods and amplitudes [26–28]. All these studies report that eggs are most successfully activated by repetitive Ca^{2+} spikes. In mouse eggs, the rate of pronucleus formation, which marks the entry of the fertilized egg into interphase before the first mitotic division, increases with the frequency of the artificially induced Ca^{2+} spikes [28]. However, oscillations of Ca^{2+} are not a prerequisite for egg activation. In mice, parthenogenetic activation by high levels of ionophore can also be achieved [29]; it is interesting to mention that activation by such a monotonous Ca^{2+} increase can only be carried out on 'old' eggs, in which the level of active MPF has started to decrease spontaneously. Equally interesting is the fact that after intracytoplasmic sperm injection of human eggs (ICSI), a non-oscillatory Ca^{2+} response is sometimes produced, and is compatible with the development of two pronuclei. No data however exist to assess the developmental potential of such zygotes [30]. In summary, it appears that in mammals early parthenogenetic development of eggs is favoured by an oscillatory pattern of Ca^{2+} increases, although such repetitive spikes are not absolutely required.

A recent study performed on rabbit oocytes provides some biochemical clue to the understanding of the role of oscillatory Ca^{2+} dynamics at fertilization in mammals. It is shown indeed that the H1 kinase activity, which directly reflects the level of active MPF, rapidly decreases after the first, artificially induced Ca^{2+} spike. However, this inactivation is only transient. Repetitive Ca^{2+} increases are necessary to keep MPF inactivated on an extended period of time [31].

In the present study, we propose a theoretical model that could account for the fact that egg activation is optimized by an oscillatory Ca^{2+} signal. We assume that Ca^{2+} oscillations are generated independently from the cell cycle oscillator, but that Ca^{2+} affects the behaviour of the cell cycle at various levels. The model is based on the activation of CaMKII by cytosolic Ca^{2+}. The latter activated protein in turn possesses a dual role: on one hand, it triggers a decrease in CSF activity at each Ca^{2+} spike and on the other hand, active CaMKII indirectly induces MPF inactivation through a CSF-independent pathway. As the molecular mechanisms by which CaMKII governs MPF and CSF inactivation still remains to be

elucidated, we assume in the present study that the different processes occurring in response to Ca^{2+} elevations are brought about by a cascade of post-translational modifications. The dual effect of Ca^{2+} on MPF activity (direct or mediated by CSF) is at the basis of the temporal pattern of MPF inactivation reproduced by the model; although a few Ca^{2+} spikes suffice to decrease transiently MPF activity, MPF can be kept inactivated for an extended period of time only if the total number of Ca^{2+} spikes is sufficient to bring CSF below a threshold level. The model also accounts for egg activation after ionophore application in appropriate conditions, as well as for arrest in metaphase III (MIII). The latter MIII arrest can be experimentally observed when an insufficient number of Ca^{2+} spikes is applied to the system or if a low dose of ionophore is given to a freshly ovulated egg [29]. Finally, the present analysis predicts that no cellular division can occur as long as the egg is subjected to stimulation by repetitive Ca^{2+} spikes, a property of the model which could be easily tested experimentally.

In the following, we use a model previously developed for the embryonic cell cycle in *Xenopus* oocytes [32]. Our results however remain qualitatively independent from the detailed mechanism supposed to underlie periodic variations in MPF (see Ref. [33]). On the other hand, in the numerical simulations, the Ca^{2+} spikes are generated at regular time intervals by a mathematical function, to get, in a simple way, spikes of appropriate characteristics. Any biochemical model for Ca^{2+} oscillations (see Refs. [34,35] for reviews) could also be used without altering the following results, as we do not assume any feedback of the species governing the cell cycle machinery on the mechanism generating the Ca^{2+} spikes. The important assumptions of the model concern the relationship between Ca^{2+} and MPF inactivation.

2. Model

2.1. Overview of the minimal model previously proposed for the cell cycle

Unfertilized mammalian eggs are arrested in the metaphase of the second meiosis, in a state characterized by a high level of cyclin, and thus also a high level of the dimeric complex made of $p34^{cdc2}$ kinase

and cyclin, called MPF. Here, it is assumed that except for the role of Ca^{2+}, the termination of the second meiosis is governed by the same essential biochemical processes as the metaphase-anaphase transition in the mitotic cell cycle.

The periodicity of the cell cycle relies on a biochemical oscillator in which MPF plays a central role, each division being driven by a peak in MPF activity. The grey-shaded region of Fig. 1 provides a schematical representation of the minimal model for MPF oscillations proposed previously [32], and used in the present study. The model considers three variables, namely the concentration of cyclin B (C), the fraction of active cdc2 kinase (M) and the fraction of active proteolytic complex (X). Cyclin B (C) is synthesized at a constant rate. It activates a phosphatase, called cdc25, which brings the inactive cdc2 (M^+) in an active, dephosphorylated state (M). In reality, the active species is made of a complex between cyclin B and cdc2, but the inclusion of a step accounting for the formation of such a heterodimer does not qualitatively affect the behaviour of the model [36]. Phosphorylation (deactivation) of cdc2 is mediated by the wee1 kinase. Unphosphorylated cdc2 (M) triggers the activation of a proteolytic complex (X) known as APC (anaphase promoting complex), which labels cyclins for degradation through the ubiquitin pathway. Inactivation of APC occurs through dephosphorylation by a phosphatase. The negative feedback exerted by X on the level of cyclin is at the core of the oscillatory mechanism. Autocatalytic activation of cdc2 kinase, reported by some experimental studies [37,38] and considered in other models [33], can also be incorporated in the present model but appears unnecessary for the occurrence of oscillations [39].

The temporal evolution of the three variables of the minimal model is thus given by the following ordinary differential equations (see Refs. [32,39] for a detailed presentation of the model):

$$\frac{dC}{dt} = v_i - v_d X \frac{C}{K_d + C} - k_d C \tag{1}$$

$$\frac{dM}{dt} = V_{M1} \frac{C}{K_c + C} \frac{1 - M}{K_1 + 1 - M} - V_2 \frac{M}{K_2 + M} \tag{2}$$

$$\frac{dX}{dt} = V_{M3} M \frac{1 - X}{K_3 + 1 - X} - V_4 \frac{X}{K_4 + X} \tag{3}$$

In the above equations, C represents the concentration of cyclin B and is thus expressed in μM. In contrast, M and X both represent fractions of active protein, i.e. the concentration of the active form divided by the total concentration of the protein considered. In consequence, these quantities are dimensionless and $(1 - M)$ and $(1 - X)$ represent the
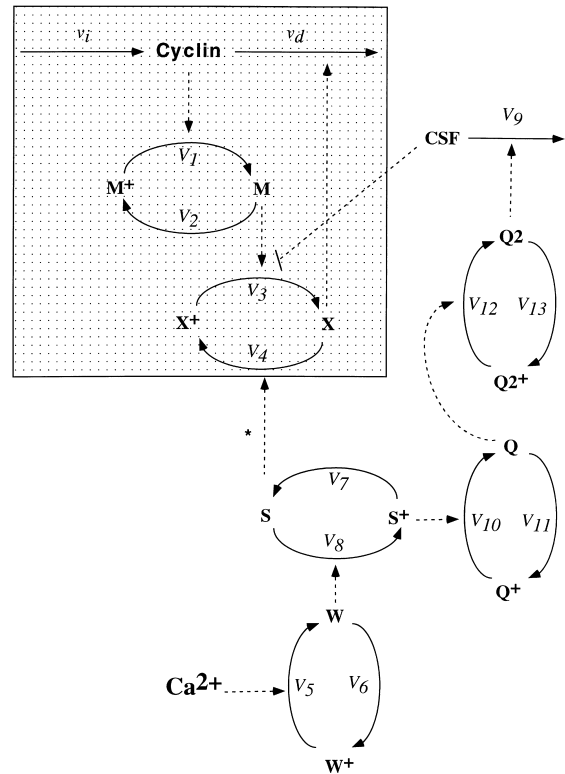

Fig. 1. Schematic representation of the mathematical model proposed to account for the effect of Ca^{2+} oscillations on MII arrested mammalian eggs. The grey-shaded region represents the model proposed previously for the early embryonic cell cycle [32]. Eggs are arrested in MII due to a high level of CSF, which inhibits the activation of the APC complex which initiates the degradation of cyclin. Ca^{2+} is supposed to activate CaMKII (W). The active form of this enzyme phosphorylates a hypothetical mediator protein (S into S^+). S deactivates the anaphase promoting complex X, while S^+ indirectly leads to CSF inactivation. The different loops represent reversible phosphorylation pathways. Dashed arrows indicate activations, while the dashed line terminated by a hyphen stands for an inhibition. C stands for cyclin, M for MPF, X for the ubiquitin-dependent APC and W for CaMKII. Other letters represent unknown, hypothetical protein substrates. The $^+$ indicates the inactive form of the protein in all cases, except for the mediator S for which both forms are assumed to be active in different pathways. See text for details.

fraction of inactive cdc2 kinase and of inactive APC, respectively. As to the parameters, v_i represents the constant rate of cyclin B synthesis, while v_d is its maximal degradation rate by X. K_d denotes the Michaelis constant for cyclin degradation. A non-specific degradation of cyclin B, characterized by a first order rate constant k_d, is also considered. Activation (dephosphorylation) of cdc2 kinase occurs at a maximal velocity noted V_{M1}, and is activated by cyclin through a michaelian process characterized by a constant K_c. V_2 stands for the maximal velocity of cdc2 deactivation (phosphorylation). Both V_{M1} and V_2 have been scaled by the total concentration of kinase. V_{M3} and V_4 are the scaled maximal velocities of the kinase and phosphatase supposed to activate and deactivate APC (X), respectively. The K_i (i = 1–4) represent the Michaelis constants characterizing the activation and deactivation processes, divided by the total amount of kinase (for K_1 and K_2) or of APC complex (for K_3 and K_4).

Sustained oscillations occur in the model provided that thresholds exist in the dependence of M on C, and of X on M; these sharp dependences are fulfilled as long as all the K_i's are considerably smaller than 1. Oscillations in the level of cyclin B, MPF and APC complex as obtained with the model defined by Eq. (1) Eq. (2) Eq. (3) are shown in Fig. 2A. These oscillations can be suppressed by appropriate changes in the maximal velocities characterizing the diverse activation and deactivation processes [39,40].

Unfertilized mature eggs are arrested in a state of high cyclin and MPF because CSF prevents the degradation of cyclin. Of particular interest for modelling the MII arrest in the system defined by Eqs. (1), (2) and (3) is the fact that decreasing the maximal velocity of activation of the APC complex (V_{M3}) in the model described above, allows the system to quit the oscillatory domain; a steady state characterized by high levels of both cyclin and MPF is then established (Fig. 2B; see also Ref. [38]). As to the mammalian MII arrest, we assume that CSF inhibits the transformation of the APC complex into an active form. This inhibition could be indirect, i.e. CSF could have an effect at various stages of the ubiquitin pathway, but, for sake of simplicity, we consider that CSF directly inhibits the transformation of X^+ into X (see Fig. 1). In the following, the situation shown in Fig. 2B will be considered as an initial condition for

studying the effect of an oscillatory Ca^{2+} signal on MII arrested eggs.

2.2. Full model for the resumption of the cell cycle in MII arrested eggs: rationale

The model proposed to account for the Ca^{2+}-induced relief of mammalian eggs from MII arrest is schematized in Fig. 1. As mentioned above, the grey-shaded region represents the minimal mechanism pre-
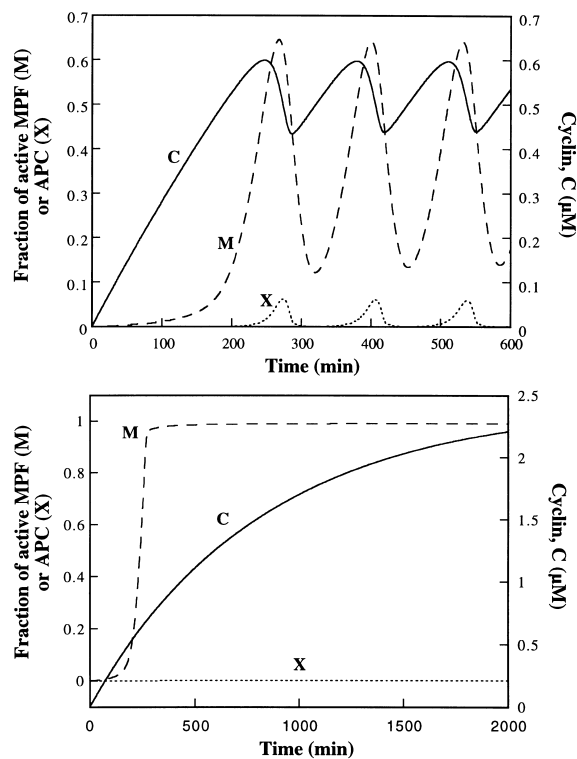

Fig. 2. (A) Sustained oscillations of cyclin, active MPF and active APC in the minimal model for the cell cycle [32]. Results have been obtained by numerical integration of Eqs. (1), (2) and (3) with the following parameter values: $v_i = 0.003$ μM min^{-1}, $v_d = 0.18$ μM min^{-1}, $K_d = 0.05$ μM, $k_d = 0.0012$ min^{-1}, $V_{M1} = 0.36$ min^{-1}, $K_c = 0.5$ μM, $V_2 = 0.186$ min^{-1}, $V_{M3} = 0.072$ min^{-1}, $V_4 = 0.048$ min^{-1}, $K_1 = K_2 = K_3 = K_4 = 0.005$. The total concentrations of MPF and APC are both supposed to be equal to 4 μM. (B) Arrest of the cell cycle in a state characterized by high levels of cyclin and active MPF, and by a low level of APC complex X, which corresponds to the situation observed in MII arrest. Cyclin concentration also evolves to a stable steady state ($C = 2.4$ μM). Results have been obtained by numerical integration of Eq. (1), (2) and (3) with the same parameter values as in (A), except for $V_{M3} = 0.0045$ min^{-1}.

viously proposed to account for periodic MPF activity [32]; the remaining part indicates how Ca^{2+} and CSF are supposed to affect this oscillatory activity. It is assumed that Ca^{2+} and CSF both interfere with the cell cycle machinery by affecting the cyclin degradation pathway, i.e. the characteristics of the reversible phosphorylation loop of the APC complex noted X.

The first assumption is that CSF inhibits the transformation of X into the active state. To consider that CSF activity has reached its maximum in the mature egg ready to be fertilized, we assume in the model that CSF is initially at a high arbitrarily chosen value, and that this level can only decrease in response to Ca^{2+}. There is no renewal of CSF once fertilization has occurred. The latter level of CSF inhibits cyclin degradation. An increase in cytosolic Ca^{2+} then deactivates CSF: according to experimental results [19,21, 41], it is assumed that Ca^{2+} activates CaMKII (W),

which itself triggers the activation of a hypothetical protein substrate, called S. The latter species must be viewed as a still unidentified 'mediator' between CaMKII and the activity of the APC complex. The phosphorylated form of this substrate, denoted S^+, triggers the degradation of CSF through two reversible phosphorylation loops. These loops introduce time-delays in the model, a phenomenon that will allow us to account for the observation that CSF is inactivated well after MPF (see below).

In principle, the latter model (i.e. Fig. 1 in which the dashed line marked * is ignored) could account on its own for the fact that a sufficient increase in cytosolic Ca^{2+} can resume the cell cycle. After an appropriate Ca^{2+} increase indeed, the inhibition of APC activation would be relieved and the cell cycle machinery could resume. It can be intuitively foreseen, however, that this mechanism in which CSF is
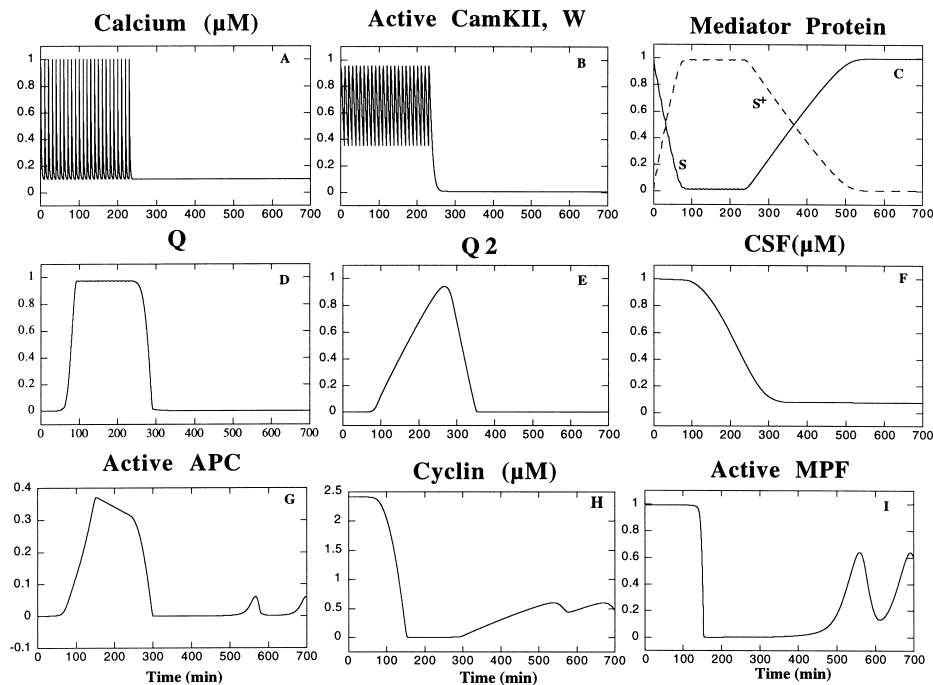

Fig. 3. Numerical simulation of the full model for the resumption of the cell cycle schematized in Fig. 1. Results have been obtained by numerical integration of the system defined by Eqs. (1), (2), (4)–(9) using a simplified mathematical definition of the Ca^{2+} dynamics (see text for details). Parameters values are the same as in Fig. 2A with $V'_{M3} = 0.072$ min^{-1}, $V'_{M4} = 0.048$ min^{-1}, $K_I = 0.5$ μM, $V_5 = 8.0$ min^{-1}, $V_6 = 0.2$ min^{-1}, $K_5 = K_6 = 1$, $K_A = 0.7$ μM, $W_T = 10$ μM, $V_7 = 0.0045$ min^{-1}, $V_{M8} = 0.03$ min^{-1}, $K_7 = K_8 = 0.05$, $V_{M9} = 0.015$ μM min^{-1}, $K_9 = 0.5$, $k_9 = 0.0001$ min^{-1}, $V_{M10} = 0.2$ min^{-1}, $V_{M11} = 0.14$ min^{-1}, $V_{M12} = 0.02$ min^{-1}, $V_{M13} = 0.014$ min^{-1}, $K_{10} = K_{11} = K_{12} = K_{13} = 0.01$, $S_T = Q_T = Q_{2T} = 1$ μM. The Ca^{2+} dynamics is characterized by a period equal to 10 min, a basal level and a maximal amplitude equal to 0.1 and 1 μM, respectively, a half-width for exponential decay equal to 1.5 min and a total number of spikes equal to 24. The Ca^{2+}-independent decrease in CSF (term $-k_9 \, CSF$ in Eq. (8)) begins at time 0, i.e. simultaneously with the onset of the first Ca^{2+} spike.

the only brake to cell cycle resumption is not able to account for at least three main experimental observations. First, such a model would predict that the decrease in MPF activity always follows that in CSF, while the opposite sequence is experimentally observed [13,14]. Second, such a scheme cannot explain why, in rabbit oocytes, the Ca^{2+}-induced decrease in the level of active MPF is only transient if the number of Ca^{2+} spikes applied to the egg is too low [31]. Finally, this system cannot account for the so-called MIII arrest, a pathological state resulting from an incomplete activation of the egg [29,42]. In this case indeed, extrusion of the second polar body is observed, a phenomenon which reflects a decrease in the level of MPF activity, but, afterwards, a new metaphase spindle is formed, suggesting that MPF activity has risen again; this arrested egg can be reactivated.

The second assumption of the model is that there is some CSF-independent pathway for egg activation by Ca^{2+}. The central idea of the full model is to assume that CaMKII has a dual role, and affects the level of active APC both indirectly through CSF inactivation and directly through activation of the APC complex (see Fig. 1). We thus consider that the mediator S, whose phosphorylation finally results in CSF inactivation, also possesses some intrinsic activity when it is unphosphorylated: the transformation of the APC from its active (X) to its inactive (X^+) form is assumed to be activated by the unphosphorylated form of the mediator. As S is high in the absence of Ca^{2+} and decreases in response to Ca^{2+} spikes, increasing cytosolic Ca^{2+} triggers a decrease in the rate of inactivation of X. The resulting higher level of active APC in turn triggers cyclin degradation. This mechanism provides a rapid and CSF-independent control of the level of active MPF by cytosolic Ca^{2+}.

2.3. Mathematical equations of the full model

In addition to the three variables of the basic cell cycle model, five other variables need to be considered in the full model. As the detailed kinetics of the events occurring at cell cycle resumption is far from being identified, the model is phenomenological. The dynamics of activation–deactivation of CaMKII (W) is described by a reversible phosphorylation loop, the interconversion between both forms being catalyzed by a kinase and a phosphatase acting with Michaelis–

Menten kinetics [24,43]. Thus, the evolution of the fraction of active CaMKII is given by the following differential equation:

$$\frac{dW}{dt} = V_5 \frac{1-W}{K_5 + 1 - W} - V_6 \frac{W}{K_6 + W} \tag{4}$$

in which

$$V_5 = V_{M5} \frac{Z^4}{K_A^4 + Z^4}$$

In these equations, W is defined as the concentration of CaMKII in the active form, with W_T being the total amount of protein substrate. The fraction of inactive CaMKII is thus given by $(1 - W)$. Moreover, V_{M5} and V_6 denote the effective maximal rates of the kinase and the phosphatase, divided by W_T; K_5 and K_6 are the normalized Michaelis constants of the two latter enzymes. K_A denotes the threshold constant of activation of the kinase by cytosolic Ca^{2+}. The Hill coefficient taken as equal to 4 allows for the observed high level of cooperativity in the activation of CaMKII by Ca^{2+} [44].

Active CaMKII (W) triggers the phosphorylation of S into S^+. Thus:

$$\frac{dS}{dt} = V_7 \frac{1-S}{K_7 + 1 - S} - V_8 \frac{S}{K_8 + S} \tag{5}$$

in which $V_8 = V_{M8} W$ where S represents the fraction of unphosphorylated mediator protein. V_7 and V_{M8} denote, respectively, the maximal rates of phosphorylation and dephosphorylation, divided by the total amount of substrate (S_T). K_7 and K_8 are the normalized Michaelis constants associated with these processes.

The phosphorylated form of S (S^+) allows another protein to become active. If Q_T is the total concentration of this substrate, Q and Q^+ ($= 1 - Q$) represent the fraction of protein into the active and inactive state, respectively. The evolution of the fraction of substrate in the active form is given by:

$$\frac{dQ}{dt} = V_{10} \frac{1-Q}{K_{10} + 1 - Q} - V_{11} \frac{Q}{K_{11} + Q} \tag{6}$$

in which $V_{10} = V_{M10} (1 - S)^4$

V_{M10} and V_{11} indicate, respectively, the maximal rates of activation and inactivation, divided by Q_T. K_{10} and K_{11} are the normalized Michaelis constants associated with these processes. Activation of Q by

the phosphorylated form of the mediator S is assumed to be highly cooperative. In the same manner,

$$\frac{dQ_2}{dt} = V_{12} \frac{1 - Q_2}{K_{12} + 1 - Q_2} - V_{13} \frac{Q_2}{K_{13} + Q_2} \tag{7}$$

in which $V_{12} = V_{M12} Q$

Parameters related to Eq. (7) have been defined in the same manner as in Eq. (6).

The ultimate effect of the pathway defined by Eq. (4) Eq. (5) Eq. (6) Eq. (7) is to trigger CSF inactivation. This phenomenon is supposed to obey the following kinetics:

$$\frac{dCSF}{dt} = -V_{M9} Q_2 \frac{CSF}{K_9 + CSF} - k_9 CSF \tag{8}$$

where V_{M9} stands for the maximal velocity of CSF inactivation and K_9 is the half-saturation constant of this process. We also assume that CSF can be inactivated in a Ca^{2+}-independent manner with first-order kinetics (k_9). This term, which is much smaller than the Ca^{2+}-activated degradation of CSF, reflects that, as time goes on, less Ca^{2+} is needed to activate the egg; following Eq. (8) indeed, the level of CSF will spontaneously decrease, thus allowing the APC complex to slowly reactivate. For simplicity, the level of CSF activity is represented by the concentration of the still unknown species assumed to play that role.

Finally, we have to transform Eq. (3), which gives the evolution of the fraction of active APC complex, to incorporate the regulations of its activation–deactivation loop by CSF and by the unphosphorylated mediator S. Eq. (3) becomes:

$$\frac{dX}{dt} = V_3 \frac{1 - X}{K_3 + 1 - X} - V_4 \frac{X}{K_4 + X} \tag{9}$$

in which

$$V_3 = V'_{M3} M \frac{K_i^4}{K_i^4 + CSF^4} \quad \text{and} \quad V_4 = V'_{M4} S$$

K_i stands for the constant characterizing the inhibition by CSF of APC activation.

Eqs. (1), (2), (4)–(9) represent a system of eight ordinary differential equations which can be numerically integrated. In the simulations, fertilization is assumed to correspond to the time at which Ca^{2+} is increased in a stepwise manner up to a fixed, maximal amplitude. Ca^{2+} is then decreased following an exponential law back to its basal level. This artificial

procedure to generate a Ca^{2+} spike is repeated periodically. The Ca^{2+} dynamics is thus characterized by a resting level $[Ca^{2+}]_0$, a maximal amplitude A, a period T and a half-time for exponential decay from A to $[Ca^{2+}]_0$, τ.

3. Numerical simulations of Ca^{2+}-induced relief from metaphase II arrest in mammalian eggs

After fertilization, mouse oocytes display Ca^{2+} oscillations with a period typically equal to 10 min, although a high variability can be observed among different individuals of the same species [27]. These oscillations can last for up to 4 h. Fig. 3A shows the temporal pattern of repetitive Ca^{2+} spikes which has been chosen to mirror the physiological situation (24 Ca^{2+} spikes of 1 μM amplitude, with a periodicity of 10 min and a half-time for exponential decay equal to 1.5 min). According to Eq. (4), these repetitive Ca^{2+} increases lead to successive spikes in the level of activated CaMKII (Fig. 3B). The high level of cooperativity in CaMKII activation by Ca^{2+} allows the fraction of active CaMKII to follow the same temporal pattern as the level of Ca^{2+}. It is important to note that CaMKII does not return to basal activity between two successive Ca^{2+} spikes; this is due to the fact that V_6 has been taken smaller than V_5 (i.e. the rate of dephosphorylation of CaMKII is low, as compared to the rate of phosphorylation). Such a partial deactivation of CaMKII is important in the behaviour of the full model, as we will see below. These peaks in CaMKII activity in turn induce the progressive transformation of S into S^+ (see Eq. (5) and Fig. 3C); the maximal velocity of the latter transformation is such that only a small fraction of this mediator protein can be converted in response to a Ca^{2+} peak (low value of V_{M8} as compared to the Ca^{2+} dynamics). Moreover, it is assumed that the system has no time to reverse between two spikes, a phenomenon which allows the CSF degradation pathway to integrate the total number of Ca^{2+} spikes. The absence of transformation of S^+ into S between two Ca^{2+} spikes is due both to the assumption that V_7 is smaller than V_{M8} and to the fact that the fraction of CaMKII in the active form remains relatively high (about 0.4) between two Ca^{2+} spikes.

Crucial to the behaviour of the model is the fact that

the CaMKII-induced changes in the balance between the S and S^+ form of the mediator has two effects. First, the decrease in the fraction of substrate in the S form directly affects the activity of the APC complex (X), responsible for cyclin degradation (Fig. 3G). As S decreases, the balance between the active (X) and inactive (X^+) forms of the APC complex switches towards the active form. As a direct result, the level of cyclin drops (Fig. 3H), and consequently, the level of MPF (Fig. 3I). This stage corresponds to the entry of the fertilized egg in interphase. On the other hand, the increase in the amount of mediator in the S^+ form leads to a progressive decrease in CSF activity (Fig. 3F). Owing to the existence of two reversible phosphorylation loops between S^+ and the decline in CSF activity (see Fig. 3D for Q and Fig. 3E for Q_2), CSF inactivation is delayed with respect to the primary Ca^{2+} increases. Finally, when both CSF activity and

Fig. 4. Stability diagram of the minimal model for the cell cycle defined by Eq. (1)–(3), in the (V_4, V_{M3}) parameter space. These maximal velocities characterize, respectively, deactivation and activation of the APC complex. The evolution of the full, eight-variable model in the same conditions as in Fig. 3 is successively represented by four points referred to as (1) to (4). (1) is the initial state of the system in MII arrest, characterized by a high level of CSF and a basal level of Ca^{2+}. (2) represents the situation after eight Ca^{2+} spikes. APC has been activated, allowing the active MPF to de-crease and the egg to enter in interphase. CSF is still active. (3) represents the situation after 20 Ca^{2+} spikes; CSF is inactivated. (4) represents the state of the system once Ca^{2+} oscillations have stopped. This state is oscillatory, corresponding to the resumption of the cell cycle. The points indicated (3′) and (4′) stand for the situation simulated in Fig. 5, in which the number of Ca^{2+} spikes is not sufficient to restart the cell cycle. The values of the variables at the various points have been obtained by numerical integration of the full model.

Ca^{2+} have come down to their basal levels, MPF can rise again and induce the first mitosis of the embryo.

The complex dynamics of this eight-variable system can be better understood when resorting to the analysis shown in Fig. 4. There, the region of oscillations in the minimal, three-variable cell cycle model (defined by Eq. (1)–(3)) is shown as a function of V_{M3} and V_4 (see also Ref. [40]). The other variables of the full model interfere with the minimal model through these two maximal velocities characterizing the reversible phosphorylation loop of the APC complex (X). Thus, different typical situations of the full model can be visualized in this V_{M3}/V_4 stability diagram, thus allowing for a qualitative understanding of the dynamics of the eight-variable system. In fact, to visualize a given state of the full model in the stability diagram of the three-variable model, one has to consider that V_{M3} is given by

$$V'_{M3} \frac{K_i^4}{K_i^4 + CSF^4}; \text{ and } V_4 \text{ is given by } V'_{M4}S.$$

The values of CSF and S are numerically evaluated at various characteristic stages. The initial state of the system simulated in Fig. 3 corresponds to a MII arrested egg characterized by a high level of CSF (1 μM) and a basal level of Ca^{2+} (0.1 μM). In such a state, S is high. The location of this point in the stability diagram (point (1) in Fig. 4) corroborates the fact that this state is stable and characterized by a low value of the fraction of active APC complex (X) and a high value of active MPF (M). Fertilization is simulated by applying to the system a series of Ca^{2+} spikes which repetitively activate CaMKII. Their first effect is to decrease S (and thus V_4). After this rapid decline, the state of the system corresponds to the point marked (2) in the stability diagram. This point is just on the opposite side of the oscillatory domain and corresponds to a stable state with a high fraction of active APC complex (X) and a low level of active MPF. This situation is reminiscent of what is observed during interphase. The second and slower effect of the Ca^{2+} spikes is to gradually decrease CSF activity. Thus, the value of V_{M3} progressively increases up to the point marked (3) in the stability diagram. The corresponding levels of cyclin, APC complex (X) and MPF are not significantly altered by the latter change. In contrast, when the Ca^{2+} spikes finally stop, V_4 rapidly increases again up to the point (4)

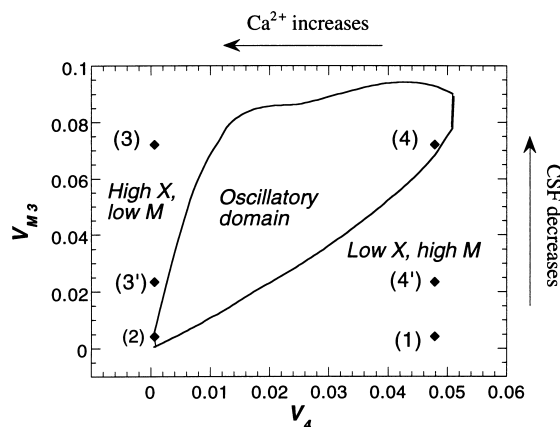which is in the oscillatory domain and thus corresponds to the resumption of the cell cycle.

The results shown in Fig. 3 have been obtained when assuming that most loops in the model (M, X, S, Q and Q_2) exhibit a threshold-like behaviour. In Fig. 3, these thresholds originate from the fact that the various kinases and phosphatases act in their region of zero-order kinetics [43], meaning that the enzymes are saturated by their substrates. Other assumptions as high levels of cooperativity or the inclusion of intermediate loops could however much relax these constraints on the parameter values, at the expense of an increased complexity of the model.

4. Effect of the number, frequency and amplitude of Ca²⁺ spikes

4.1. Reducing the number of spikes at a given frequency

The theoretical model presented above can be used to investigate how the number of Ca^{2+} spikes affects the evolution of MPF. In Fig. 5, the number of Ca^{2+} spikes has been reduced as compared to the situation shown in Fig. 3 (14 spikes in Fig. 5 as against 24 in Fig. 3); the period of Ca^{2+} oscillations remains
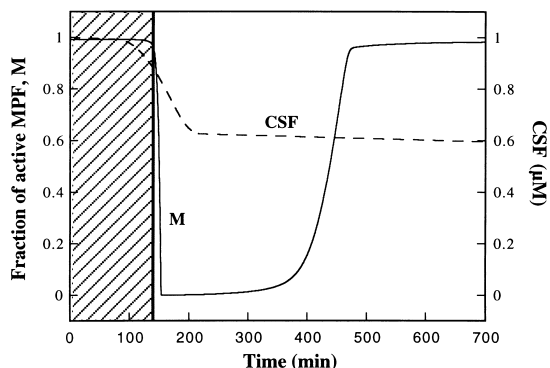

Fig. 5. Simulation of MIII arrest in an egg which has been stimulated by an insufficient number of Ca^{2+} spikes. The dashed region shows the time during which the system has been stimulated by repetitive Ca^{2+} increases with a periodicity of 10 min. MPF activity (plain line) decreases in response to Ca^{2+} spikes, but, as the number of Ca^{2+} spikes is too low, CSF activity (dashed line) does not decline to the basal level. Thus, MPF activity rises again when Ca^{2+} oscillations stop. Results have been obtained as in Fig. 3, except for the fact that the total number of Ca^{2+} spikes characterizing the Ca^{2+} dynamics is here taken as equal to 14.

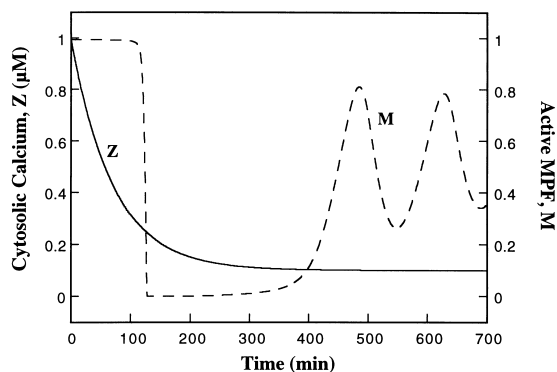Fig. 6. Simulation of cell cycle resumption by a unique, long-lasting Ca^{2+} spike. The evolution of cytosolic Ca^{2+} is shown by the plain line, while the dashed line indicates the corresponding evolution of the level of active MPF. Results have been obtained as in Fig. 3, except for the fact that the number of Ca^{2+} spikes characterizing the Ca^{2+} dynamics is here equal to 1 and that the half-time for the exponential decay of this spike is taken as equal to 70 min.

unchanged. In the case of a low number of Ca^{2+} spikes, although MPF drops after eight Ca^{2+} spikes, this decline is only transient. The fraction of active MPF progressively rises back to a stable, elevated level when Ca^{2+} returns to its steady-state value. The dashed line in Fig. 5 indicates that CSF has only decreased by ~40% in response to 14 Ca^{2+} spikes, which explains the high stable level of active MPF. This situation is reminiscent of both the transient decrease in active MPF observed, in vitro, in rabbit eggs [31] and of the MIII arrest reported in vivo for mouse eggs [29]. From a theoretical point of view, one can understand this behaviour by resorting to the stability diagram shown in Fig. 4. In this figure, the points representative of the simulation shown in Fig. 5 are indicated by (1), (2), (3′) and (4′). Because of an insufficient CSF inactivation (i.e. a too low increase in V_{M3} from (2) to (3′)), the system does not end up in an oscillatory state when Ca^{2+} returns to its basal level.

Experiments performed with Ca^{2+} ionophores indicate that mature eggs can sometimes be activated in response to one Ca^{2+} spike. Such a situation can in principle be accounted for by the model, as shown in Fig. 6. In this figure, the half-time for exponential decay of the level of cytosolic Ca^{2+} is 70 min. A detailed numerical investigation of the behaviour of the model shows that, to decrease CSF back to the basal level and thus to allow for irreversible cell

cycle resumption, Ca^{2+} has to remain elevated above a threshold value of 0.5 μM for 70 min (either continuously, or repetitively with a period which is short as compared to the intrinsic evolution of the APC complex (X), as we will see below). From a physical point of view, such a sustained Ca^{2+} increase would be lethal for the cell. In the model, a Ca^{2+} spike of much shorter duration can however activate the egg if it is assumed that the initial level of CSF activity is lower than in Fig. 3 (not shown). The latter situation could correspond to an 'older egg', in which the level of CSF has spontaneously declined, due to some endogenous protease activity. In that respect, it is interesting to mention that, in some cases, old eggs can even spontaneously activate. In summary, the present simulations suggest that egg activation by a non-oscillatory Ca^{2+} increase can be obtained either with a long-lasting stimulation by Ca^{2+}, or by assuming that CSF activity at time of activation is low, as it could be the case in old eggs.

4.2. Varying the frequency or the amplitude of the repetitive Ca^{2+} spikes

The effect of changing the frequency or the amplitude of Ca^{2+} oscillations is shown in Fig. 7. Two aspects must be considered. First, one can compute the time necessary to decrease MPF, which would correspond to the entry in interphase. In Fig. 7A, Ca^{2+} spikes of various frequencies are applied to the system. There is no restriction in the number of spikes, i.e. the latter are applied as long as necessary to inactivate MPF. In this case, the time to decrease MPF increases in a roughly exponential manner with the period of Ca^{2+} oscillations. The latter relation reflects the balance between activation and deactivation in the various loops involved in the transduction pathway between Ca^{2+} and cyclin degradation. As long as during a spike Ca^{2+} remains above the threshold value for CaMKII activation, the results are barely affected by the amplitude of oscillations. These results can be compared with the experiments performed by Ozil and Swann [28] in which they varied the period of artificially induced Ca^{2+} spikes in mouse oocytes; in that system, the time for the pronucleus to become visible, a phenomenon which marks the entry in interphase, and thus the decline in the level of MPF, clearly increases in parallel with the period of the Ca^{2+} spikes. No attempt was made in the latter experiments to vary the amplitude of these artificially induced Ca^{2+} oscillations.

Second, one can compute the time between the first Ca^{2+} spike and the first peak in MPF, which would correspond to the first mitosis, as a function of the period of Ca^{2+} oscillations. In Fig. 7B, it is considered that the system is stimulated during 4 h by Ca^{2+} spikes of various frequencies. In consequence, the total number of spikes also varies from one numerical simula-
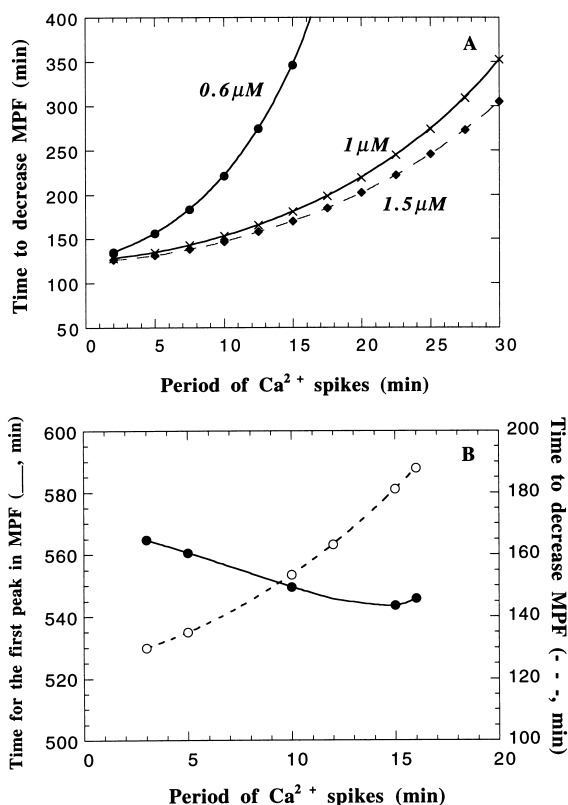

Fig. 7. Theoretical investigation of the influence of the Ca^{2+} dynamics on the kinetics of cell cycle resumption after fertilization. (A) shows the influence of the period of Ca^{2+} spiking on the time at which the level of active MPF drops. This stage corresponds to the entry of the activated egg in interphase. The various curves have been obtained for different amplitudes of Ca^{2+} spiking, as indicated. Ca^{2+} spikes are applied for 600 min. (B) shows the influence of the period of Ca^{2+} spiking on the time at which MPF reaches its first maximum, after the initial drop. This stage would correspond to the first mitosis. Ca^{2+} spikes are only applied during 4 h, which implies that the total number of Ca^{2+} spikes varies with the period. For comparison, the time taken for the first drop in MPF in these conditions (slightly different from (A)) is also indicated (dashed line). Results have been obtained as in Fig. 3.

tion to the other. The reason why such a 'protocol' has been adopted (and not the same as in Fig. 7A) is that, in our simulations, there is no cell cycle resumption as long as Ca^{2+} is spiking, as it will be discussed in Section 4.3. Fig. 7B clearly shows that the time laps between the onset of stimulation and the first peak in MPF is little affected (~4%) by the frequency of the Ca^{2+} spikes. This time interval is merely imposed by the time taken by the cyclin to increase after the return of Ca^{2+} to its basal level, i.e. after the 4 h of stimulation. The time taken by cyclin to increase is itself dictated by the choice of parameter values characterizing the kinetics of the cell cycle but is practically independent of the parameters characterizing the preceding Ca^{2+} dynamics. In fact, the time for the first peak in MPF slightly decreases when the period of Ca^{2+} oscillations increases because the final level of CSF activity increases in parallel with the period, due to the fact that the total number of Ca^{2+} spikes received by the system during 4 h becomes lower. The final rate of APC activation (V_3) is thus lower when the period of Ca^{2+} oscillations is larger. The latter change somewhat accelerates the increase in cyclin.

For comparison, the time needed for the initial decrease in the level of active MPF in response to activation by Ca^{2+} is also shown in Fig. 7B. This rela-
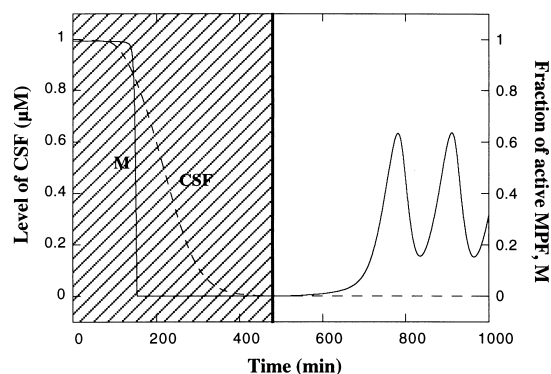

Fig. 8. Theoretical prediction of the model for cell cycle resumption schematized in Fig. 1: the time for the first mitosis is delayed when the egg receives a number of Ca^{2+} spikes that largely exceeds the number that is necessary for activation. Here, the egg is assumed to be activated during 8 h (with Ca^{2+} spikes of 10 min periods); as compared with the similar situation in which the number of Ca^{2+} spikes is equal to 24 (Fig. 3), the time for the first mitosis is delayed of about 4 h. Results have been obtained as in Fig. 3, except for the number of Ca^{2+} spikes which here equals 48.

tionship is not exactly the same as in Fig. 7A because in Fig. 7B, Ca^{2+} spikes are only applied during 4 h. The model thus predicts that the time taken by the egg to enter in interphase or to undergo the first division are differently affected by the Ca^{2+} dynamics. Pronucleus formation is accelerated when the frequency of the Ca^{2+} spikes is increased. In contrast, the time for the first division remains roughly independent from this frequency.

4.3. Increasing the number of Ca^{2+} spikes at a given frequency

An interesting property of the present model is that it suggests that the level of MPF cannot increase in the presence of a high level of Ca^{2+}, even in the absence of CSF activity as Ca^{2+} indirectly increases the activity of the APC complex (see Fig. 1). Furthermore, oscillations in the level of cyclin and active MPF can only occur when the Ca^{2+} level is low. This property can be understood by looking at the stability diagram shown in Fig. 4. There, it can be seen that oscillations cannot occur for low values of V_4, which correspond to minimal values of the mediator protein in the S form, and thus to maximal Ca^{2+} concentrations. Thus, numerical simulations of the model schematized in Fig. 1 predict that the time required for resumption of the cell cycle will increase if the total stimulation time by Ca^{2+} is extended. The latter prediction is illustrated in Fig. 8. In comparison to Fig. 3, the number of Ca^{2+} spikes has been doubled (with the same frequency): simulations show a delay of nearly 4 h in the appearance of the first peak in MPF, as compared to Fig. 3. Such a prediction could be tested experimentally by activating the eggs by a very large number of artificial Ca^{2+} spikes.

Two experimental observations indirectly corroborate the latter theoretical prediction. First, it has been reported that after fertilization of mouse oocytes, Ca^{2+} oscillations cease during entry in interphase, at the time when pronuclei are forming [45]. The second relevant observation comes from ascidian eggs, although the activation process is somewhat different in this species. In a recent study, the intracellular Ca^{2+} level has been measured simultaneously with histone H1 activity [46]; it appears that, at the second meiosis, MPF activity increases after the arrest of the Ca^{2+} spikes.

5. Discussion

In the present study, a model which qualitatively accounts for the Ca^{2+}-induced relief from MII arrest at fertilization of mammalian eggs has been developed. The central idea of the model is that the elevated Ca^{2+} level first overcomes inhibition of cyclin degradation by CSF, and later induces CSF inactivation. Activation of both pathways is mediated by CaMKII. Thus, the model assumes that the oscillatory level of CaMKII that follows the Ca^{2+} spikes has two effects, characterized by different time-scales. The first pathway simply counteracts the CSF-mediated arrest by directly activating the APC complex which initiates cyclin degradation, an effect that disappears when Ca^{2+} returns to its basal level. The second, irreversible and slow process activated by CaMKII is the inactivation of CSF. Thus, upon combination of these two effects, Ca^{2+} oscillations first decrease the level of active MPF, which allows the egg to enter in interphase, and later inactivate CSF. When CSF is sufficiently low and when Ca^{2+} oscillations stop, the egg can undergo the first mitosis.

Noteworthy is the fact that the model presented here remains qualitative. No attempt has been made to closely match the time scales of the events occurring in the simulations in response to Ca^{2+} spikes, with the experimentally determined time laps in the early development of the eggs from any mammalian species. Also the concentrations of the various chemical species appearing in the model have been chosen rather arbitrarily. A quantitative approach would indeed be premature both because some parts of the model are speculative and because the kinetics of the events occurring between CaMKII activation by Ca^{2+} and the decrease in MPF is largely unknown. The aim of the study is both to provide a mechanism that can qualitatively account for many experimental observations and to emphasize the fact that the temporal pattern of early activation by Ca^{2+} clearly affects the developmental potentiality of the egg (see also the article by J.-P. Ozil in this issue).

The understanding of the role of the Ca^{2+} changes at fertilization is of great interest, particularly in the view that it might provide some insights into the causes of unsuccessful in vitro fertilization procedures in humans [47]. Although the present model is the first one to specifically investigate the link between Ca^{2+} oscillations and resumption of the cell cycle at fertilization, the relations between Ca^{2+} and the mitotic cell cycle have already been approached in a theoretical manner. As in the present model, these theoretical studies assume that CaMKII activates the degradation of cyclin. The first model relates the dynamics of cytosolic Ca^{2+} to progression through mitosis, G_1 and G_2 phase of the cell cycle, on the basis of the assumption that high levels of MPF trigger the release of $InsP_3$ [48,49]. In that study, the Ca^{2+} dynamics is tightly coupled to the cell cycle oscillator, with a one to one peak correlation between Ca^{2+} and MPF. Such a situation cannot account for the coexistence between a basal level of Ca^{2+} and a high level of active MPF, as seen in MII arrested eggs, nor for the fact that numerous Ca^{2+} spikes are necessary for the egg to enter in interphase after fertilization.

Another theoretical investigation of the role of Ca^{2+} in the early embryonic cell cycle suggests that Ca^{2+} oscillations drive MPF activation cycles [50]. Interestingly, the authors suggest that the Ca^{2+} dynamics could be autonomously oscillatory, while the MPF system would be excitatory or bistable. In that scheme, Ca^{2+} is assumed to activate both cyclin degradation and phosphorylation of cdc25, the phosphatase responsible for MPF activation. In the absence of additional assumptions, this model cannot account for the relief from MII arrest in response to a Ca^{2+} increase, as Ca^{2+} cannot induce an initial decrease in MPF activity in the presence of a high level of inhibition of cyclin degradation by CSF. However, it must be stressed that various relations between the Ca^{2+} dynamics and the MPF oscillator most probably prevail in different situations; in particular, it is reasonable to assume that mitosis is not regulated in the same manner as resumption of meiosis at fertilization.

Given the lack of experimental data, some of the regulatory pathways introduced in the model have been chosen rather arbitrarily. Other regulations could indeed lead to a behaviour similar to the one presented in Fig. 3. For example, the APC inactivation by the unphosphorylated form S of the mediator (V_4 on Fig. 1) could be substituted by the assumption that the Ca^{2+}-activated CaMKII in fact inhibits MPF activation (V_1 on Fig. 1). This possibility has been discarded because an opposite effect, namely the activation of cdc25 by Ca^{2+}, has been reported by an in vitro experimental study [51]. In the same manner, the rather

complex sequence of loops leading to a slow inactivation of CSF can be transformed into a CaMKII-activated, slow degradation of CSF which is inhibited by *M*. The reason why we have favoured the first possibility (sequence of activation–deactivation loops) is that MIII arrest is very difficult to simulate with the second pathway. Finally, that CaMKII can autophosphorylate and thus act as a biochemical switch [52] is another possibility that could explain the transition from a stable to an oscillatory MPF system. Again, we have not favoured this possibility on the basis that the variations in the level of MPF activity have to be reversible quite rapidly (MIII arrest or mitotic cell cycle).

In contrast, some assumptions of the model cannot be removed without affecting drastically the qualitative behaviour of the model. In particular, the results shown in Fig. 3 imperatively depend on the assumption that CaMKII has two different effects on the cell cycle. Moreover, the effect of Ca^{2+} on CSF activity has to be slow and irreversible, while the pathway that can overcome CSF-mediated arrest must be faster and reversible. Until now, there is no experimental evidence in favour of the existence of two different pathways targeted by CaMKII at egg activation.

In a first approximation, we have neglected any possible feedback of the cell cycle on the Ca^{2+} dynamics. Although such an effect most probably occurs [4,15,17], its inclusion in a theoretical model would be quite complex as it appears from the experimental data that it is mainly the reorganization of the microtubular network associated with the early development of the egg that interferes with the Ca^{2+} dynamics. Moreover, the interplay between the cell cycle machinery and the mechanism for Ca^{2+} release is bidirectional. Of particular interest in that respect is the observation that CaMKII might be associated with the spindle and could, in consequence be activated only as long as the latter microtubular organization remains intact [17].

The present model provides an example of a system in which an oscillatory pattern of stimulation optimizes the cellular response in the absence of any frequency coding. This optimization in fact stems from the natural constraints of the system: to respond properly, the system indeed needs the long-lasting presence of the stimulus to fully deactivate CSF. Given the regulatory properties of the Ca^{2+} dynamics inside the cell, such a sustained increase in the level of Ca^{2+} is most successfully approached by oscillations. Although rapid Ca^{2+} spiking accelerates the activation process, there appears to be a large range of frequencies able to activate the egg. In that respect, the model recovers the experimental observation that egg activation is a very robust phenomenon which appears to be unaffected by large variations in the oscillatory pattern of Ca^{2+} increases.

Acknowledgements

References

[1] L. Jaffe, Dev. Biol. 99 (1983) 265.
[2] D. Kline, J. Kline, Dev. Biol. 149 (1992) 80.
[3] K. Swann, J.-P. Ozil, Int. Rev. Cytol. 152 (1994) 183.
[4] A. McDougall, C. Sardet, Curr. Biol. 5 (1995) 318.
[5] J. Parrington, K. Swann, V. Shevchenko, A. Sesay, F. Lai, Nature 379 (1996) 364.
[6] S. Miyazaki, J. Cell Biol. 106 (1988) 345.
[7] G. Dupont, O. McGuinness, M. Johnson, M.J. Berridge, F. Borgese, Biochem. J. 316 (1996) 583.
[8] P. Snow, D. Yim, J. Leibow, S. Sainiand, R. Nuccitelli, Dev. Biol. 180 (1996) 108.
[9] K. Foltz, J. Partin, W. Lennarz, Science 259 (1993) 1421.
[10] A. Murray, T. Hunt, The Cell Cycle: An Introduction, Oxford University Press, Oxford, 1993.
[11] M. Glotzer, A. Murray, M. Kirschner, Nature 349 (1991) 132.
[12] N. Sagata, N. Watanabe, G. Vande Woude, Y. Ikawa, Nature 342 (1989) 512.
[13] N. Watanabe, T. Hunt, Y. Ikawa, N. Sagata, Nature 352 (1991) 247.
[14] M.-H. Verlhac, J. Kubiak, H. Clarke, B. Maro, Development 120 (1994) 1017.
[15] J. Kubiak, M. Weber, H. de Pennart, N. Winston, B. Maro, EMBO J. 12 (1993) 3773.
[16] R. Moses, D. Kline, Dev. Biol. 171 (1995) 111.
[17] N. Winston, O. McGuinness, M. Johnson, B. Maro, J. Cell Sci. 108 (1995) 143.
[18] M.-H. Verlhac, J. Kubiak, M. Weber, G. Géraud, W. Colledge, M. Evans, B. Maro, Development 122 (1996) 815.

[19] T. Lorca, F. Cruzalegui, D. Fesquet, J. Cavadore, J. Méry, A. Means, M. Dorée, Nature 366 (1993) 270.
[20] N. Morin, A. Abrieu, T. Lorca, F. Martin, M. Dorée, EMBO J. 13 (1994) 4343.
[21] Z. Xu, L. Lefevre, T. Ducibella, R. Schultz, G. Kopf, Dev. Biol. 180 (1996) 594.
[22] P. Rapp, M.J. Berridge, J. Exp. Biol. 93 (1981) 119.
[23] T. Meyer, L. Stryer, Annu. Rev. Biophys. Biophys. Chem. 20 (1991) 153.
[24] G. Dupont, A. Goldbeter, Biophys. Chem. 42 (1992) 257.
[25] Y. Tang, H. Othmer, Proc. Natl. Acad. Sci. USA 92 (1995) 7869.
[26] J.-P. Ozil, Development 109 (1990) 117.
[27] A. Vitullo, J.-P. Ozil, Dev. Biol. 151 (1992) 128.
[28] J.-P. Ozil, K. Swann, J. Physiol. 483.2 (1995) 331.
[29] C. Vincent, T. Cheek, M. Johnson, J. Cell Sci. 103 (1992) 383.
[30] J. Tesarik, Hum. Reprod. 9 (1994) 977.
[31] P. Collas, T. Chang, C. Long, J. Robl, Mol. Reprod. Dev. 40 (1995) 253.
[32] A. Goldbeter, Proc. Natl. Acad. Sci. USA 88 (1991) 9107.
[33] J. Tyson, Proc. Natl. Acad. Sci. USA 88 (1991) 7328.
[34] G. Dupont, A. Goldbeter, BioEssays 14 (1992) 485.
[35] J. Sneyd, J. Keizer, M. Sanderson, FASEB J. 9 (1995) 1463.
[36] P.-C. Romond, J.-M. Guilmot, A. Goldbeter, Ber. Bunsenges. Phys. Chem. 98 (1994) 1152.
[37] M. Cyert, M. Kirschner, Cell 53 (1988) 185.
[38] U. Strausfeld, J. Labbé, D. Fesquet, J. Cavadore, A. Picard, K. Sadhu, P. Russell, M. Dorée, Nature 351 (1991) 242.
[39] A. Goldbeter, Comments Theoret. Biol. 3 (1993) 75.
[40] A. Goldbeter, J.-M. Guilmot, J. Phys. Chem. 100 (1996) 19174.
[41] T. Lorca, A. Abrieu, A. Means, M. Dorée, Biochim. Biophys. Acta 1223 (1994) 325.
[42] J. Kubiak, Dev. Biol. 136 (1989) 537.
[43] A. Goldbeter, D. Koshland, Proc. Natl. Acad. Sci. USA 78 (1981) 6840.
[44] H. Schulman, in: P. Greengard, G.A. Robison (Eds.), Advances in Second Messenger and Phosphoprotein Research, Vol. 22, Raven Press, New York, 1988, p. 39.
[45] K. Jones, J. Carroll, J. Merriman, D. Whittingham, T. Kono, Development 121 (1995) 3259.
[46] G. Russo, K. Kyozuka, L. Antonazzo, E. Tostiand, B. Dale, Development 122 (1996) 1995.
[47] S. Homa, J. Carroll, K. Swann, Hum. Reprod. 8 (1993) 1274.
[48] I. Baran, BioSystems 33 (1994) 203.
[49] I. Baran, Biophys. J. 70 (1996) 1198.
[50] C. Swanson, A. Arkin, J. Ross, Proc. Natl. Acad. Sci. USA 94 (1997) 1194.
[51] M. Whitaker, R. Patel, Development 108 (1990) 525.
[52] T. Meyer, P. Hanson, L. Stryer, H. Schulman, Science 256 (1992) 1199.